Journal of Chromatography, 194 (1980) 1–10
Elsevier Scientific Publishing Company, Amsterdam — Printed in The Netherlands

CHROM. 12,720

FREE DISPLACEMENT ELECTROPHORESIS (ISOTACHOPHORESIS): AN ABSOLUTE DETERMINATION OF THE KOHLRAUSCH FUNCTIONS AND THEIR USE IN INTERACTION STUDIES

S. HJERTÉN*, L.-G. ÖFVERSTEDT and G. JOHANSSON
Institute of Biochemistry, University of Uppsala, Biomedical Centre, Box 576, S-751 23 Uppsala (Sweden)
(Received January 28th, 1980)

SUMMARY

The Kohlrausch regulating functions (the ω-functions) have been calculated for the moving zones in carrier-free displacement electrophoresis (isotachophoresis) experiments. We verified experimentally that the ω-functions of the different migrating zones have the same value at the steady state. From studies of the Kohlrausch functions it is easy to decide whether interaction between the constituents of a zone occurs.

INTRODUCTION

The theory of electrophoretically displaced boundaries was outlined by Kohlrausch in 1897[1]. Kohlrausch introduced the ω-function ("die beharrliche Funktion"), defined as $\omega = \Sigma c_j/m_j$, where c_j is the concentration and m_j the mobility of the ion j. Kohlrausch derived mathematically that the ω-function has the same value in two phases separated by an electrophoretically moving boundary. In spite of the great importance of this statement in theoretical treatments of all kinds of electrophoresis methods, to the best of our knowledge, no experiments to verify it have been published. The reason could be the lack of electrophoresis techniques that permit accurate, simultaneous measurements of the concentrations c_j and the mobilities m_j. The electrophoresis apparatus used has some unique features that render it very suitable for such measurements (see Discussion). For reasons also given under Discussion we chose to determine the Kohlrausch functions in displacement electrophoresis (isotachophoresis) experiments.

THEORETICAL

Only the theory of displacement electrophoresis that is of interest for our verification experiments is given here. For a more exhaustive treatment, see refs. 2 and 3.

0021-9673/80/0000–0000/$02.25

The electrophoretic mobility of an ion is defined as its velocity at unit field strength:

$$m = v/E \tag{1}$$

where m = mobility ($m^2/Vsec$), v = velocity (m/sec) and E = electrical field strength (V/m)*.

The field strength can be expressed as

$$E = \frac{I}{A\kappa} = \frac{i}{\kappa} \tag{2}$$

where I = current (A), A = cross-sectional area (m^2), κ = conductivity ($\Omega^{-1}m^{-1}$) and i = current density (A/m^2).

Combination of eqns. 1 and 2 provides the mobility equation:

$$m = \frac{vA\kappa}{I} \tag{3}$$

which often is used for the calculation of ion mobilities.

The determination of counter-ion mobility demands further consideration. The procedure is as follows. The current density in a solution is a function of the ion concentrations and velocities:

$$i = F\Sigma c_j z_j v_j \tag{4}$$

F = Faraday's constant $\approx$ 96 488 A·sec/equiv., c_j concentration of the ion j (mol/m^3) and z_j = charge of the ion j (equiv./mol) (z and v, as well as m in eqn. 3, are given positive signs for cations and negative signs for anions).

Consider a zone α consisting of an ion L and a counter ion R (Fig. 1). (We assume that we perform the experiments at an intermediate pH where the contribu-

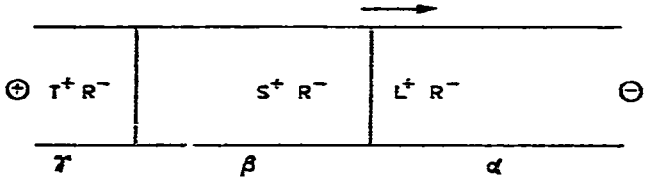

Fig. 1. Schematic representation of displacement electrophoresis at the steady-state. The leading zone α, the sample zone β and the terminating zone γ consist of the cations L^+, S^+ and T^+, respectively, and the common counter ion R^-. The arrow indicates the direction of migration of the boundaries between the zones.

* CGS or MKS units are often used in papers dealing with the fractionation and characterization of biological material. As this paper is of a physical character we have employed SI units, which are commonly used in physics.

tions from H^+ and OH^- to the Kohlrausch function are negligible.) Then, according to eqn. 4

$$i = F(c_L z_L v_L + c_R z_R v_R) \tag{5}$$

Electroneutrality demands that

$$c_L z_L + c_R z_R = 0 \tag{6}$$

Combination of eqns. 1, 5 and 6 gives

$$i = F c_L z_L E(m_L - m_R) \tag{7}$$

Introduction of eqn. 2 gives a function suitable for the calculation of counter-ion mobility:

$$m_R = m_L - \frac{\kappa}{F c_L z_L} \tag{8}$$

The ω-functions of the zones α, β and γ in Fig. 1 can be determined from the mobility values (eqns. 3 and 8), and the measured ion concentrations and their valencies:

$$\omega^\alpha = \frac{c_L z_L}{m_L} + \frac{c_R^\alpha z_R}{m_R^\alpha} \tag{9a}$$

$$\omega^\beta = \frac{c_S z_S}{m_S} + \frac{c_R^\beta z_R}{m_R^\beta} \tag{9b}$$

$$\omega^\gamma = \frac{c_T z_T}{m_T} + \frac{c_R^\gamma z_R}{m_R^\gamma} \tag{9c}$$

The ratio of the ω-functions for the two zones α and β can be calculated either directly from eqns. 9a and 9b or from the following equation, obtained by combining eqns. 9a, 9b, 3, 8 and 6:

$$\frac{\omega^\alpha}{\omega^\beta} = \frac{\kappa^\beta}{\kappa^\alpha} \cdot \frac{\dfrac{I}{c_S z_S} - FvA}{\dfrac{I}{c_L z_L} - FvA} \tag{10a}$$

A similar equation for the zones α and γ is obtained by combining eqns. 9a, 9c, 3, 8 and 6:

$$\frac{\omega^\alpha}{\omega^\gamma} = \frac{\kappa^\gamma}{\kappa^\alpha} \cdot \frac{\dfrac{I}{c_T z_T} - FvA}{\dfrac{I}{c_L z_L} - FvA} \tag{10b}$$

These equations were also used to estimate the uncertainty in the calculated values of the ω-function ratio (see Table II).

The values of the ω-functions in parentheses in Tables IIa and IIb were calculated from eqns. 9a and 9b, putting $m_R^\alpha = m_R^\beta =$ the arithmetic mean of the measured counter-ion mobilities in the zones α and β, and in Table IIc from eqns. 9a and 9c, putting $m_R^\alpha = m_R^\gamma =$ the mean value of the counter-ion mobilities in the zones α and γ.

EXPERIMENTAL

Reagents

All chemicals [potassium acetate, cobalt(II) acetate, copper(II) acetate, acetic acid and hydrochloric acid] were of pro analisi purity. Tris(hydroxymethyl)aminomethane (Tris) and 5-sulphosalicylic acid (SSA) were purified by recrystallization in 40% ethanol.

Apparatus

All experiments were carried out in the free solution electrophoresis equipment previously described in detail[4–6]. The electrophoresis chamber was a 40-cm long, slowly rotating horizontal quartz tube with an inner diameter of approximately 2.5 mm. The rotation has been shown to give efficient stabilization against convectional disturbances. A syringe pump was connected to one electrode vessel, making it possible to apply a controlled liquid flow in the electrophoresis tube. The apparatus was equipped with a photoelectric scanning device, giving the ultraviolet absorption pattern of the zones on the strip chart of a recorder. The scanning wavelength was 280 nm; the background absorption at 320 nm was automatically subtracted by means of a rotating filter.

Loading the electrophoresis tube

The left electrode vessel and half of the tube were filled with leading buffer with the aid of a syringe. A sample zone about 10 cm long (*ca.* 0.5 ml) was applied in contact with the leading buffer while the tube was rotating. The remainder of the tube and the right electrode vessel were then filled with terminating buffer.

Electrophoresis

After the electrophoresis current had been switched on, a counterflow of leading buffer was applied to keep the front boundary of the sample zone stationary in the tube, permitting complete adaptation of the sample zone concentration to the leading zone. The steady-state sample concentration was considered to be reached when the scanner trace showed that the concentration was constant throughout the zone and no further change in zone length could be detected (Fig. 2). The counterflow was turned off and the migration distance of a moving boundary was then determined by scanning the tube at accurately measured time intervals (the position P of a boundary was taken as the point of the boundary that corresponded to half the height of the scanning trace; see Fig. 2b). The migration velocity thus obtained for one boundary is equal to those of all other boundaries (as they all move with the same speed when the steady state has been attained). The runs were performed at 20 °C.

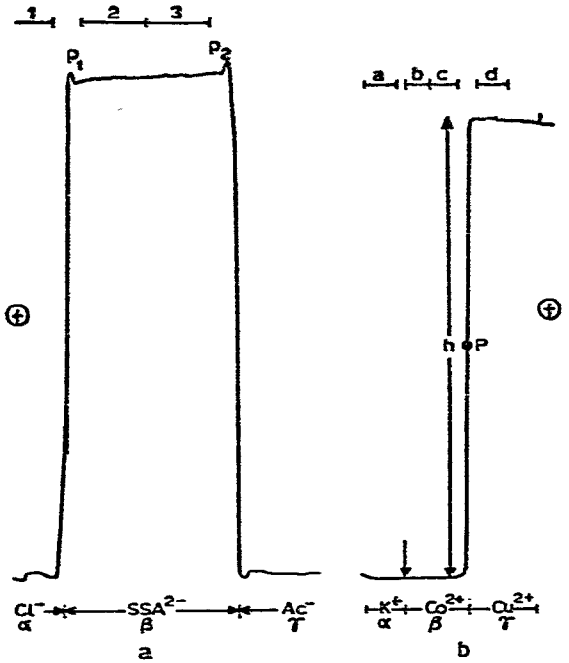

Fig. 2. Strip-chart recorder traces of scans of the electrophoresis tube at 280 nm. The ions of the zones are indicated below the curve. (a) Anionic system, Cl^-–SSA^{2-}–Ac^- with $Tris^+$ as counter ion; (b) cationic system, K^+–Co^{2+}–Cu^{2+} with Ac^- as counter ion. Recovered fractions are marked by numbers 1–3 and letters a–d.

Collection of fractions

When the front boundary of the sample zone had reached the end of the tube, the voltage was switched off and the zones were collected, starting with the terminating solution. Each zone was withdrawn with a dry syringe.

The absorbances of the collected fractions were measured with a Beckman ACTA CIII spectrophotometer at wavelengths of 297, 510 and 760 nm for SSA^{2-} (the anion of 5-sulphosalicylic acid), Co^{2+} and Cu^{2+}, respectively. Standard graphs of absorbance against concentration were constructed at the pH of the zones.

The conductivities were measured with a Radiometer CDM3 conductivity meter, equipped with a CDC314 microcell.

RESULTS

One anionic and one cationic system were investigated.

Anionic system

The leading solution consisted of hydrochloric acid and Tris in the molar ratio 1:2, ensuring maximal buffering capacity and good reproducibility. The pH obtained was 8.3 at 20 °C. Three concentrations of leading solution were analysed (see Table Ia). 5-Sulphosalicylic acid (SSA) was used as the sample (the sample applied was prepared from the acid and Tris in the molar ratio 1:4). At pH 8.3

the acid appears almost completely as SSA^{2-} since $pK_2 \approx 3$ and $pK_3 \approx 11$. The sample concentration used was close to the expected steady-state concentration. The terminating solution consisted of HAc and Tris, Tris initially being at the same concentration as in the hydrochloric acid–Tris buffer in the leading solution.

Electrophoresis was performed as described above. After 2-4 h the concentrations in the sample zone had become adapted to those of the leading zone and the concentrations in the terminating zone to those of the sample zone. Fig. 2a shows the recorder trace of a scan of the tube. The SSA zone could easily be detected by its UV absorbance. The small peaks p_1 and p_2 at the zone boundaries in Fig. 2a were probably due to light deviation caused by refractive index differences between the zones (Schlieren effects). Neither the leading chloride zone nor the terminating acetate zone showed any absorbance at 280 or 320 nm.

The migration velocity of the front boundary of the SSA zone was determined. The standard deviation of this determination was very low, as shown in Fig. 3. The slope (= migration velocity) was calculated by the method of least squares.

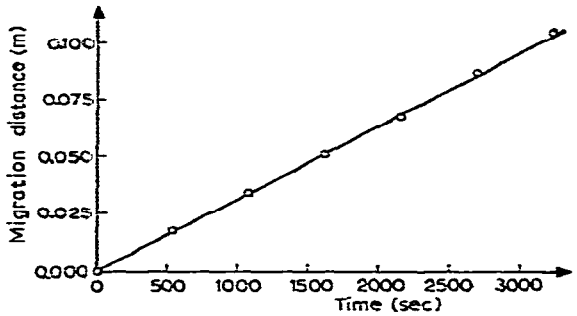

Fig. 3. Migration distance of the boundary between the Cl^- zone and the SSA^{2-} zone of the anionic system (see Fig. 2a) at different times. The migration distance of the boundary was obtained from the scanning pattern on the recorder chart.

When the electrophoresis was completed, the contents of the tube were withdrawn in fractions 1–3, as indicated in Fig. 2a. The conductivity of each fraction and the SSA concentration in fraction 2 were determined, and their measured values are listed in Table Ia. The ion mobilities and the values of the ω-function of the different zones were calculated from these values by eqns. 3, 8 ,9 and 10 (see Table IIa). For the calculation of the Kohlrausch regulating functions we used both the calculated mobilities of the counter ion and their arithmetic means. The values of the ω-functions in parentheses in Tables IIa, IIb and IIc refer to the mean values. When comparing the ω-functions in Table II it is more suitable to consider those calculated from the mean values of the mobilities because these functions according to the treatment given in refs. 1 and 7, have the same value only if the mobility of an ion is the same in both phases.

Cationic system

KAc–HAc (pH 5.40) was chosen as the leading solution and $CuAc_2$–HAc (pH 5.10) as the terminating solution. The applied sample contained $CoAc_2$ and

TABLE I

EXPERIMENTALLY DETERMINED PARAMETERS

(a) The Cl^- (α) and SSA^{2-} (β) zones (see Fig. 2a):

$^cCl^-$ (mol/m³)	κ^α $(\Omega m)^{-1}$	$^cSSA^{2-}$ (mol/m³)	κ^α $(\Omega m)^{-1}$	$I \cdot 10^3$ (A)	$v \cdot 10^5$ (m/sec)	$A \cdot 10^6$ (m²)
25.0	0.206	11.3	0.145	0.495	3.22	4.56
50.0	0.386	22.2	0.253	2.48	8.15	4.56
100	0.734	43.3	0.484	4.99	7.93	4.56

(b) The K^+ (α) and Co^{2+} (β) zones (see Fig. 2b):

$^cK^+$ (mol/m³)	κ^α $(\Omega m)^{-1}$	$^cCo^{2+}$ (mol/m³)	κ^β $(\Omega m)^{-1}$	$I \cdot 10^3$ (A)	$v \cdot 10^5$ (m/sec)	$A \cdot 10^6$ (m²)
100	0.800	37.5	0.404	2.44	2.52	6.25
200	1.55	74.7	0.689	4.90	2.70	6.25

(c) The K^+ (α) and Cu^{2+} (γ) zones (see Fig. 2b):

$^cK^+$ (mol/m³)	κ^α $(\Omega m)^{-1}$	$^cCu^{2+}$ (mol/m³)	κ^γ $(\Omega m)^{-1}$	$I \cdot 10^3$ (A)	$v \cdot 10^5$ (m/sec)	$A \cdot 10^6$ (m²)
100	0.800	46.5	0.238	2.44	2.52	6.25
200	1.55	100	0.369	4.90	2.70	6.25

HAc in concentrations approximately equal to the steady-state concentrations. Two leading ion concentrations were used, namely 100 and 200 mol/m³ (see Tables Ib and Ic). The counter-flow was applied for 2–4 h. Fig. 2b shows the scanner trace. The Cu zone could easily be detected by its UV absorbance. The Co zone showed no UV absorbance, but was easily localized by its red colour. The zone length could therefore be measured manually with a ruler. The position of the boundary between the leading K zone and the Co zone (indicated in Fig. 2b by an arrow) was established by such a measurement. The fractions that were analysed are indicated as a–d.

The migration velocity was calculated in the same way as for the anionic system; the boundary between Co and Cu was used for this calculation. The measured parameters of the cationic system are listed in Tables Ib and Ic. The related calculated mobility and ω-function values are presented in Tables IIb and IIc.

Error analysis

All possible care has taken to minimize the errors in the measurements. The uncertainty of a measured physical parameter consists of a standard deviation of the measurement and a systematic error related to experimental procedures. The latter was estimated according to the precision of the equipment. The limits of the errors of the calculated mobilities and ω-functions in Tables IIa, IIb and IIc were estimated using the equation

$$\frac{\Delta f}{f} = \sqrt{\sum_i \left(\frac{(\Delta f)i}{f}\right)^2} \qquad (11)$$

TABLE II

CALCULATED PARAMETERS, INCLUDING THE ω-FUNCTIONS

(a) The Cl^- (α) and SSA^{2-} (β) zones (see Fig. 2a):

$^cCl^+$ (mol/m³)	(Eqn. 3) $m_{Cl^-}\cdot 10^8$ (m²/V·sec)	(Eqn. 8) $m_{Tris^+}\cdot 10^8$ (m²/V·sec)	(Eqn. 3) $m_{SSA^{2-}}\cdot 10^8$ (m²/V·sec)	(Eqn. 8) $m_{Tris^+}\cdot 10^8$ (m²/V·sec)	(Eqn.9a) $\omega^\alpha\cdot 10^{-9}$ (mol·V·sec/m⁵)	(Eqn. 9b) $\omega^\beta\cdot 10^{-9}$ (mol·V·sec/m⁵)	(Eqn. 10a) $\omega^\alpha/\omega^\beta$
25.0 ± 0.13	−6.10 ± 0.19	2.44 ± 0.15	−4.30 ± 0.13	2.34 ± 0.17	1.44 ± 0.06 (1.46)	1.49 ± 0.09 (1.47)	0.96 ± 0.06 (0.99)
50.0 ± 0.25	−5.78 ± 0.18	2.22 ± 0.15	−3.79 ± 0.12	2.12 ± 0.15	3.12 ± 0.14 (3.17)	3.26 ± 0.20 (3.22)	0.96 ± 0.06 (0.99)
100.0 ± 0.5	−5.32 ± 0.16	2.29 ± 0.14	−3.51 ± 0.11	2.28 ± 0.15	6.25 ± 0.25 (6.26)	6.27 ± 0.35 (6.26)	1.00 ± 0.06 (1.00)

(b) The K^+ (α) and Co^{2+} (β) zones (see Fig. 2b):

$^cK^+$ (mol/m³)	$m_{K^+}\cdot 10^8$ (m²/V·sec)	$m_{Ac^-}\cdot 10^8$ (m²/V·sec)	$m_{Co^{2+}}\cdot 10^8$ (m²/V·sec)	$m_{Ac^-}\cdot 10^8$ (m²/V·sec)	$\omega^\alpha\cdot 10^{-9}$ (mol·V·sec/m⁵)	$\omega^\beta\cdot 10^{-9}$ (mol·V·sec/m⁵)	$\omega^\alpha/\omega^\beta$
100 ± 2	5.16 ± 0.18	−3.13 ± 0.23	2.61 ± 0.09	−2.97 ± 0.15	5.13 ± 0.31 (5.22)	5.40 ± 0.23 (5.33)	0.95 ± 0.07 (0.98)
200 ± 4	5.34 ± 0.19	−2.69 ± 0.23	2.37 ± 0.08	−2.41 ± 0.13	11.2 ± 0.7 (11.6)	12.5 ± 0.6 (12.2)	0.89 ± 0.07 (0.95)

(c) The K^+ (α) and Cu^{2+} (γ) zones (see Fig. 2b):

$^cK^+$ (mol/m³)	$m_{K^+}\cdot 10^8$ (m²/V·sec)	$m_{Ac^-}\cdot 10^8$ (m²/V·sec)	$m_{Cu^{2+}}\cdot 10^8$ (m²/V·sec)	$m_{Ac^-}\cdot 10^8$ (m²/V·sec)	$\omega^\alpha\cdot 10^{-9}$ (mol·V·sec/m⁵)	(Eqn. 9c) $\omega^\gamma\cdot 10^{-9}$ (mol·V·sec/m⁵)	(Eqn. 10b) $\omega^\alpha/\omega^\gamma$
100 ± 2	5.16 ± 0.18	−3.13 ± 0.23	1.54 ± 0.05	−1.12 ± 0.07	5.13 ± 0.31 (6.66)	14.4 ± 0.8 (10.4)	0.36 ± 0.03 (0.64)
200 ± 4	5.34 ± 0.19	−2.69 ± 0.23	1.27 ± 0.04	−0.64 ± 0.05	11.2 ± 0.7 (12.0)	46.9 ± 3.2 (27.8)	0.24 ± 0.02 (0.43)

where $(\Delta f)i$ denotes the relative difference in f when the parameter p_i is replaced by $p_i + \Delta p_i$; $f = f(p_i)$; Δp_i is the standard error of p_i.

DISCUSSION

Method

The electrophoresis equipment that was used has the following characteristic features that make it suitable for the present investigation. (a) Electrophoresis is performed in a carrier-free solution; it is accordingly not necessary to compensate for disturbances caused by the presence of supporting media (for instance, in the form of gels of poiyacrylamide or gradients of sucrose) and viscosity-increasing agents (for instance, methylcellulose). (b) With the photoelectric scanner one can determine accurate migration velocities and easily decide when the steady state has been attained. (c) Fractions can be withdrawn after completion of a run; the conductivity and ion concentration of any zone can therefore be measured with high accuracy. (d) The power supply is equipped with a current stabilizer; variations in the temperature of the cooling water therefore have very little influence on the migration velocities of the zones[3]. (e) Electroendosmotic flow is eliminated.

In displacement electrophoresis all adapted zones migrate with the same velocity; in addition, the number if ionic species in the zones is smaller than in zone electrophoresis or moving boundary electrophoresis. The former method therefore has the advantage that it requires fewer measurements than the other two for the calculation of the ω-functions. This is the main reason why we chose to utilize the displacement technique in this investigation. The conclusions drawn from this study are, however, relevant also to zone and moving boundary electrophoresis.

That the steady state had been attained in our experiments is evident not only from the shape of the curves in Fig. 2a and b but also from the fact that the conductivities and absorbances of fractions 2 and 3 in Fig. 2a (and b and c in Fig. 2b) differed by at most 2%. In one control experiment the SSA^{2-} zone was withdrawn in eight fractions. Accurate measurements showed that the SSA concentration in the fractions deviated less than 0.5% from the arithmetic mean.

Theory

In the deduction given by Kohlrausch[1] and Longsworth[7] a prerequisite for the ω-functions to have identical values in all zones moving in an electrical field is that the mobility of an ion has the same value in the different zones. It is therefore necessary to consider the constancy of the mobilities of the counter ions (which are the only ions in our experiments, except the negligible H^+ and OH^- ions, that appear in more than one zone). Table IIa shows that the mobility of $Tris^+$ (within experimental error) has the same value in the α and β phases. The data in Table IIb indicate that it is more uncertain whether this is true for the Ac^- ion in the K^+–Co^{2+} system. It is obvious, however, that the Ac^- ion has a different mobility in the presence of Cu^{2+} than in the presence of K^+ (Table IIc). These considerations are in agreement with the experimentally found ratio between the ω-functions: in Table IIa the ratio is close to unity; Table IIb shows possibly some deviation from unity, while a very striking deviation is observed in Table IIc. It should be stressed that the ionic concentrations c_j in the calculations of the ω-functions were set equal to the

total concentration of the ion j, which is far from correct for the Ac^- ion in the Cu^{2+} zone (Table IIc).

The above great difference between the values of the ω-functions for two moving zones is due to complex formation between Cu^{2+} and Ac^- (ref. 8). Generally, one can state that significant differences between the Kohlrausch functions, calculated with the assumption that no complex formation occurs (as we have done in this paper), are an indication of molecular interactions. A closer inspection of the Kohlrausch functions may in some instances give important information about the nature of ionic complexes, particularly if ion mobilities and ion concentrations are replaced by constituent mobilities and constituent concentrations (see ref. 7).

ACKNOWLEDGEMENT

This study was financially supported by the Swedish Natural Science Research Council.

REFERENCES

1 F. Kohlrausch, *Ann. Deut. Phys. Chem.*, 62 (1897) 209–239.
2 F. M. Everaerts, J. L. Beckers and Th. P. E. M. Verheggen, *Isotachophoresis: Theory, Instrumentation, and Applications*, Elsevier, Amsterdam, 1976.
3 S. Hjertén, in G. Milazzo (Editor), *Topics in Bioelectrochemistry and Bioenergetics*, Vol. 2, Wiley, New York, 1978, pp. 87–128.
4 S. Hjertén, *Chromatogr. Rev.*, 9 (1967) 122–219.
5 S. Hjertén, *Methods Biochem. Anal.*, 18 (1970) 55–79.
6 S. Hjertén, in N. Catsimpoolas (Editor), *Methods of Protein Separation*, Vol. 29, Plenum, New York, 1976, pp. 219–231.
7 L. G. Longsworth, in M. Bier (Editor), *Electrophoresis: Theory, Methods, and Applications*, Academic Press, New York, 1959, pp. 91–136.
8 Landolt-Börnstein, *Zahlenwerte und Funktionen*, Vol. II, Part 7, Springer, Berlin, Göttingen, Heidelberg, 6th ed., 1960, p. 137.